Original Article

Preliminary exploration of the correlation between spectral computed tomography quantitative parameters and spread through air spaces in lung adenocarcinoma

Hongzheng Song, Shiyu Cui, Liang Zhang, Henan Lou, Kai Yang, Hualong Yu, Jizheng Lin

Department of Radiology, The Affiliated Hospital of Qingdao University, Qingdao, China

Contributions: (I) Conception and design: H Song, L Zhang, J Lin; (II) Administrative support: None; (III) Provision of study materials or patients: H Song, K Yang; (IV) Collection and assembly of data: L Zhang, H Lou, H Yu; (V) Data analysis and interpretation: H Song, S Cui; (VI) Manuscript writing: All authors; (VII) Final approval of manuscript: All authors.

Correspondence to: Jizheng Lin, MM. Department of Radiology, The Affiliated Hospital of Qingdao University, No. 16 Jiangsu Road, Qingdao 266003, China. Email: linjizheng@qdu.edu.cn.

Background: The invasive pattern called spread through air spaces (STAS) is linked to an unfavorable prognosis in patients with lung adenocarcinoma (LUAD). Using computed tomography (CT) signs alone to assess STAS is subjective and lacks quantitative evaluation, whereas spectral CT can provide quantitative analysis of tumors. The aim of this study was to investigate the association between spectral CT quantitative parameters and STAS in LUAD.

Methods: We retrospectively collected consecutive patients with LUAD who underwent surgical resection and preoperative spectral CT scan at our institution. The quantitative parameters included CT values at 40, 70, and 100 keV [CT40keVa/v, CT70keVa/v, and CT100keVa/v (a: arterial; v: venous)]; iodine concentration (ICa/ICv); normalized iodine concentration (NICa/NICv); and slope λHU of the spectral curve (λHUa/λHUv). Clinical and CT features of the patients were also collected. Statistical analysis was performed to identify the quantitative parameters, clinical and CT features that were significantly correlated with STAS status. We evaluated the diagnostic performance of significant factors or models which combined quantitative parameters and CT features, using the area under the curve (AUC) of the receiver operating characteristic (ROC) curve.

Results: We enrolled a total of 47 patients, with 32 positive and 15 negative for STAS. The results revealed that CT100keVa (P=0.002), CT100keVv (P=0.007), pathologic stage (P=0.040), tumor density (P<0.001), spiculation (P=0.003), maximum solid component diameter (P=0.008), and the consolidation/tumor ratio (CTR) (P=0.001) were significantly correlated with STAS status. The tumor density demonstrated a superior diagnostic capability [AUC =0.824, 95% confidence interval (CI): 0.709–0.939, sensitivity =59.4%, specificity =100.0%] compared to other variables. CT100keVa exhibited the best diagnostic performance (AUC =0.779, 95% CI: 0.633–0.925, sensitivity =78.1%, specificity =80.0%) among the quantitative parameters. Combination models were then constructed by combining the quantitative parameters with CT features. The total combined model showed the highest diagnostic efficiency (AUC =0.952, 95% CI: 0.894–1.000, sensitivity =90.6%, specificity =86.7%).

Conclusions: Spectral CT quantitative parameters CT100keVa and CT100keVv may be potentially useful parameters in distinguishing the STAS status in LUAD.

Keywords: Spread through air spaces (STAS); lung adenocarcinoma (LUAD); spectral computed tomography (spectral CT); quantitative parameters

Submitted Jul 06, 2023. Accepted for publication Oct 16, 2023. Published online Nov 13, 2023.
doi: 10.21037/qims-23-984
View this article at: https://dx.doi.org/10.21037/qims-23-984

Introduction

Lung cancer is among the most prevalent malignant tumors, with pulmonary adenocarcinoma being its most common pathological type (1,2). The World Health Organization (WHO) classification in 2015 recognized the invasion pattern known as spread through air spaces (STAS) in lung adenocarcinoma (LUAD), which involves micropapillary clusters, solid nests, or single cells spreading beyond the main tumor's edge into the air spaces (3). The prognostic importance of STAS was further confirmed by the WHO classification of 2021 (4).

STAS is a poor prognostic factor in LUAD and has been linked to reduced disease-free survival (DFS) and overall survival (OS) (5,6). Minimally invasive sublobar resection is gaining popularity as a surgical option for treating early-stage tumors (7,8). However, recent studies (9,10) have shown that STAS-positive adenocarcinomas have a higher tendency to relapse after sublobar resection. Therefore, it is not suitable for such tumors and lobectomy is preferred. Thus, preoperative determination of STAS status is crucial for selecting the most suitable surgical method to improve patient outcomes.

Unfortunately, STAS can only be identified post-operatively (11). To date, several studies have utilized preoperative computed tomography (CT) characteristics to evaluate STAS in LUAD. Studies (12-14) have found a correlation between STAS and certain CT features, such as spiculation, lobulation, and pleural indentation. Nevertheless, these CT features are subjective and lack quantitative evaluation. Spectral CT imaging can obtain the density of materials and images at different kiloelectron volt (keV) levels, which can be used for quantitative analysis of substances (15). Spectral CT has been extensively utilized in the analysis of lung cancer, exhibiting its potential value in distinguishing benign and malignant lung lesions, identifying lymph node metastasis, and distinguishing pathological grading of lung cancer (16-18).

Therefore, investigating the correlation between spectral CT quantitative parameters and STAS may facilitate preoperative diagnosis of STAS in LUAD. However, this relationship has yet to be investigated by researchers. Thus, this study aimed to explore the potential association between spectral CT quantitative parameters and STAS in LUAD. We present this article in accordance with the STARD reporting checklist (available at https://qims.amegroups.com/article/view/10.21037/qims-23-984/rc).

Methods

Patients

This retrospective study was conducted in accordance with the Declaration of Helsinki (as revised in 2013) and approved by the Ethics Committee of the Affiliated Hospital of Qingdao University (No. QYFY WZLL 28103); the requirement for individual consent for this retrospective analysis was waived. We consecutively collected patients with LUAD who underwent surgical resection at the Affiliated Hospital of Qingdao University between January 2021 and October 2022, and they were included in the study if they met the following conditions: (I) pathology-confirmed adenocarcinoma and (II) had undergone spectral CT scan within a month prior to the surgery. The exclusion criteria were as follows: (I) multiple lesions; (II) preoperative neoadjuvant therapy; and (III) incomplete pathological data. Ultimately, 47 patients (22 males and 25 females; age range, 50–71 years; mean age, 60.9±5.8 years) were included in this study. *Figure 1* shows the flow chart of patient selection.

CT examination

The Revolution CT scanner (GE Healthcare, Chicago, IL, USA) was used to perform CT scans. The scanning parameters included: tube voltage of 80 and 140 kVp instantaneous switching (0.5 ms); automatic tube current modulation was enabled; helical tube rotation time of 0.5 s; pitch of 0.992, scanning field of view of 500 mm; slice thickness and gap of 5 mm. Intravenous injections of contrast media (Omnipaque 350, GE Healthcare) were administered to patients at a rate of 3.0 mL/s, totaling 70–80 mL. Scanning for both arterial phase (AP) and venous phase (VP) were conducted at 25 and 60 s intervals, respectively, after injection of contrast media.

CT image analysis

The original data was reconstructed to produce images with

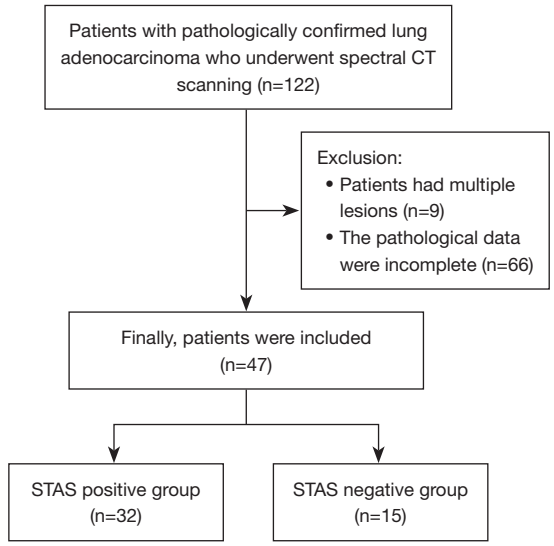

Figure 1 Flow chart of the study. CT, computed tomography; STAS, spread through air spaces.

a slice thickness of 1.25 mm. The reconstructed images were sent to an Advantage Workstation (AW4.6, GE Healthcare) and analyzed by the Gemstone Spectral Imaging (GSI) Viewer software (GE Healthcare). The images were analyzed by two radiologists with over 5 years of work experience. We selected the largest slice of the lesion to identify the region of interest (ROI), avoiding vessels, necrosis, and calcification as much as possible. CT values on 40, 70, and 100 keV monochromatic images were measured for the lesion, along with its iodine concentration (IC) on iodine-based material decomposition image. The IC of the aorta on the same slice was also measured. To minimize the effect of patient variation, the IC of the lesion was normalized to the IC of the aorta, resulting in the normalized iodine concentration (NIC). The slope of the spectral curve (λHU) was calculated as λHU = (CT40keV – CT100keV)/(100–40). The CT characteristics of the lesion, including tumor density, lobulation, spiculation, pleural indentation, and cavitation, were assessed independently by two radiologists without prior knowledge of STAS status. Any disagreements were discussed and resolved. The maximum diameter of the lesion and its solid component were measured, and the consolidation/tumor ratio (CTR) was then calculated.

Histopathologic evaluation

The definition of STAS was established as the detection of tumor cells in the pulmonary air spaces beyond the primary tumor margin (4).

Statistical analysis

The software SPSS 26.0 (IBM Corp., Armonk, NY, USA) was used for statistical analysis. Non-normally distributed continuous variables were described using medians and interquartile ranges, whereas frequencies and percentages were used to express categorical variables. Mann-Whitney *U* test or independent sample *t*-test was applied to compare continuous variables, and the χ^2 test or Fisher's exact test was employed to scrutinize categorical variables. We utilized the area under the curve (AUC) of the receiver operating characteristic (ROC) to evaluate the diagnostic efficiency of significant factors or combined models comprising CT characteristics and quantitative parameters, derived through multivariate logistic regression analysis. A two-sided P<0.05 was considered statistically significant.

Results

Patient clinical and CT characteristics

Out of the 47 identified lesions, 32 were STAS positive and 15 were STAS negative, yielding a positive STAS rate of 68.1% (32/47) as shown in *Table 1*. Pathologic stage (P=0.040), tumor density (P<0.001), spiculation (P=0.003), maximum solid component diameter (P=0.008), and CTR (P=0.001) varied significantly between the two groups, whereas the other characteristics did not demonstrate any statistically significant differences.

Quantitative parameters analysis

Table 2 displays the correlation between STAS status and quantitative parameters of spectral CT. The results indicated that CT100keVa (P=0.002) and CT100keVv (P=0.007) exhibited significant differences between the two groups. Specifically, the CT100keV values of AP and VP were significantly higher in the STAS positive group as compared to the STAS negative group. Nevertheless, no significant differences were observed between the two groups in terms of CT40keV, CT70keV, IC, NIC, and λHU for AP and VP.

Diagnostic efficiency of quantitative parameters and CT characteristics

Table 3 presents the diagnostic efficiency of each quantitative

Table 1 Clinical and CT characteristics of patients

Variable	STAS status		P value
	Negative (n=15)	Positive (n=32)	
Age (years), mean ± SD	60.5±6.3	61.0±5.6	0.786
Gender, n (%)			0.205
Female	10 (66.7)	15 (46.9)	
Male	5 (33.3)	17 (53.1)	
Smoking status, n (%)			0.503
Non-smoker	12 (80.0)	22 (68.8)	
Smoker	3 (20.0)	10 (31.3)	
T stage, n (%)			0.544
T1	12 (80.0)	20 (62.5)	
T2	3 (20.0)	11 (34.4)	
T3	0 (0.0)	1 (3.1)	
N stage, n (%)			0.179
N0	15 (100.0)	25 (78.1)	
N1	0 (0.0)	5 (15.6)	
N2	0 (0.0)	2 (6.3)	
Pathologic stage, n (%)			0.040
I	15 (100.0)	22 (68.8)	
II	0 (0.0)	8 (25.0)	
III	0 (0.0)	2 (6.3)	
Tumor density, n (%)			<0.001
pGGN	2 (13.3)	0 (0.0)	
PSN	13 (86.7)	13 (40.6)	
SN	0 (0.0)	19 (59.4)	
Lobulation, n (%)	12 (80.0)	31 (96.9)	0.089
Spiculation, n (%)	5 (33.3)	25 (78.1)	0.003
Pleural indentation, n (%)	11 (73.3)	28 (87.5)	0.245
Cavitation, n (%)	2 (13.3)	12 (37.5)	0.170
Maximum tumor diameter (mm), median (IQR)	23.20 (15.80)	22.20 (14.15)	0.349
Maximum solid component diameter (mm), median (IQR)	9.00 (14.00)	19.00 (11.00)	0.008
CTR, median (IQR)	0.45 (0.50)	0.87 (0.20)	0.001

CT, computed tomography; STAS, spread through air spaces; SD, standard deviation; pGGN, pure ground glass nodule; PSN, part solid nodule; SN, solid nodule; CTR, consolidation/tumor ratio; IQR, interquartile range.

Table 2 Association between STAS status and spectral CT quantitative parameters.

Parameters	STAS status		P value
	Negative (n=15)	Positive (n=32)	
AP			
CT40keVa (HU)	147.52 (222.89)	155.44 (80.34)	0.819
CT70keVa (HU)	10.79 (156.34)	53.01 (21.15)	0.068
CT100keVa (HU)	−3.66 (145.82)	30.46 (20.40)	0.002
ICa (100 μg/cm^3)	24.96±12.13	19.91±8.53	0.106
NICa (100 μg/cm^3)	0.27±0.12	0.21±0.09	0.064
λHUa	2.96±1.44	2.35±1.00	0.102
VP			
CT40keVv (HU)	196.11 (315.30)	186.53 (66.51)	0.945
CT70keVv (HU)	58.38 (226.79)	67.44 (25.42)	0.091
CT100keVv (HU)	22.56 (211.08)	34.92 (21.15)	0.007
ICv (100 μg/cm^3)	23.53±11.00	21.25±5.85	0.460
NICv (100 μg/cm^3)	0.61±0.26	0.54±0.16	0.363
λHUv	2.79±1.31	2.52±0.69	0.455

Data are presented as mean ± standard deviation or median (interquartile range). STAS, spread through air spaces; CT, computed tomography; AP, arterial phase; VP, venous phase; IC, iodine concentration; NIC, normalized iodine concentration; λHU, slope of the spectral curve; a, arterial; v, venous.

Table 3 Diagnostic efficiency of parameters and CT characteristics

Variables	AUC (95% CI)	Cutoff value	Sensitivity (%)	Specificity (%)
CT100keVa (HU)	0.779 (0.633–0.925)	16.875	78.1	80.0
CT100keVv (HU)	0.746 (0.605–0.886)	39.765	43.8	100.0
Tumor density	0.824 (0.709–0.939)	–	59.4	100.0
Spiculation	0.724 (0.560–0.888)	–	78.1	66.7
Maximum solid component diameter (mm)	0.743 (0.585–0.901)	15.400	71.9	73.3
CTR	0.802 (0.660–0.944)	0.798	71.9	86.7

CT, computed tomography; AUC, area under the curve; CI, confidence interval; CTR, consolidation/tumor ratio; a, arterial; v, venous.

parameter and CT characteristic, whereas *Figure 2* depicts their corresponding ROC curves. According to the findings, the tumor density demonstrated a superior diagnostic capability (AUC =0.824, 95% confidence interval (CI): 0.709–0.939, sensitivity =59.4%, specificity =100.0%) compared to other variables. Furthermore, the diagnostic performance of the quantitative parameter CT100keVa (AUC =0.779, 95% CI: 0.633–0.925, sensitivity =78.1%, specificity =80.0%) surpassed that of CT100keVv (AUC =0.746, 95% CI: 0.605–0.886, sensitivity =43.8%, specificity =100.0%).

Diagnostic efficiency of the combined models

A radiological model was created by conducting the stepwise logistic regression on the significant CT features, and the model consisted of tumor density and spiculation. These significant quantitative parameters, separately

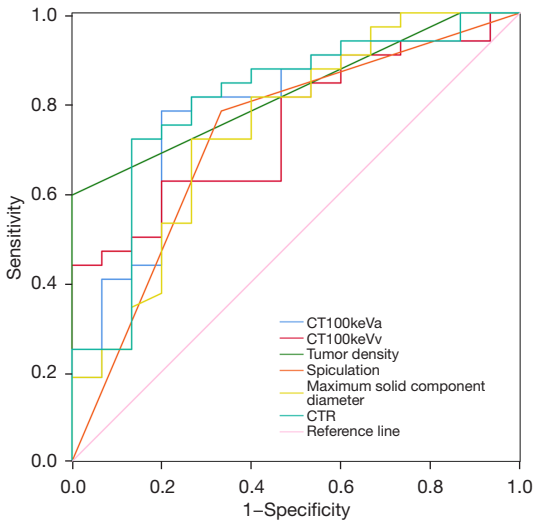

Figure 2 ROC curves of each CT quantitative parameter and CT characteristic. CT, computed tomography; a, arterial; v, venous; CTR, consolidation/tumor ratio; ROC, receiver operating characteristic.

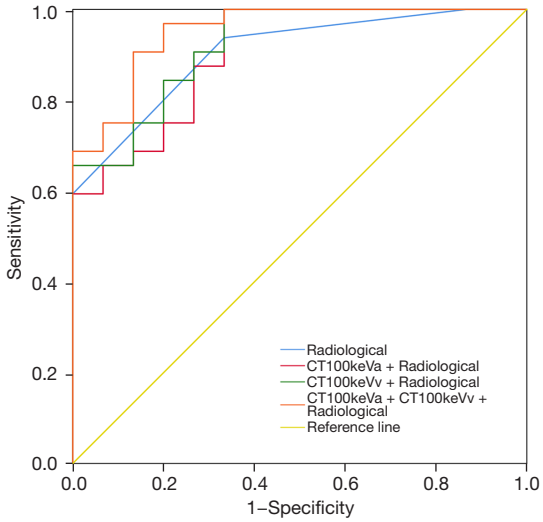

Figure 3 ROC curves of each combined model. CT, computed tomography; a, arterial; v, venous; ROC, receiver operating characteristic.

Table 4 Diagnostic efficiency of the different combined models.

Combined model	AUC (95% CI)	Cutoff value	Sensitivity (%)	Specificity (%)
Radiological	0.905 (0.821–0.989)	0.444	93.8	66.7
CT100keVa + radiological	0.904 (0.815–0.993)	0.414	100.0	66.7
CT100keVv + radiological	0.921 (0.843–0.999)	0.410	100.0	66.7
CT100keVa + CT100keVv + radiological	0.952 (0.894–1.000)	0.645	90.6	86.7

AUC, area under the curve; CI, confidence interval; CT, computed tomography; a, arterial; v, venous.

combined with the radiological model, were then used to develop the combined models. *Figure 3* displays the ROC curves for all combined models. The diagnostic efficiency of these models was superior to that of individual parameters and CT features, and the CT100keVa + CT100keVv + Radiological model showed the highest diagnostic capability (AUC =0.952, 95% CI: 0.894–1.000, sensitivity =90.6%, specificity =86.7%) (*Table 4*). *Figures 4*,*5* display two examples of spectral CT images.

Discussion

The study findings revealed a significant correlation between STAS phenomenon and the spectral CT quantitative parameters CT100keVa and CT100keVv. The STAS-positive group had significantly higher CT100keVa and CT100keVv values compared to the STAS-negative group. Additionally, combining significant quantitative parameters with CT features demonstrated a good predictive value for STAS in LUAD (AUC =0.952). This suggests that spectral CT quantitative parameters are a valuable supplement to conventional CT features that can aid clinicians in preoperative determination of STAS status in LUAD.

STAS is a novel invasive modality that serves as a significant factor contributing to the unfavorable prognosis of LUAD. Several previous studies (19-21) have demonstrated that STAS is linked to aggressive clinicopathological features including pleural invasion, high-grade histological type, and lymphovascular invasion. Tumors that exhibit STAS positivity display more invasive ability and a faster growth rate. These phenomena indicate that STAS-positive tumors may require a greater blood

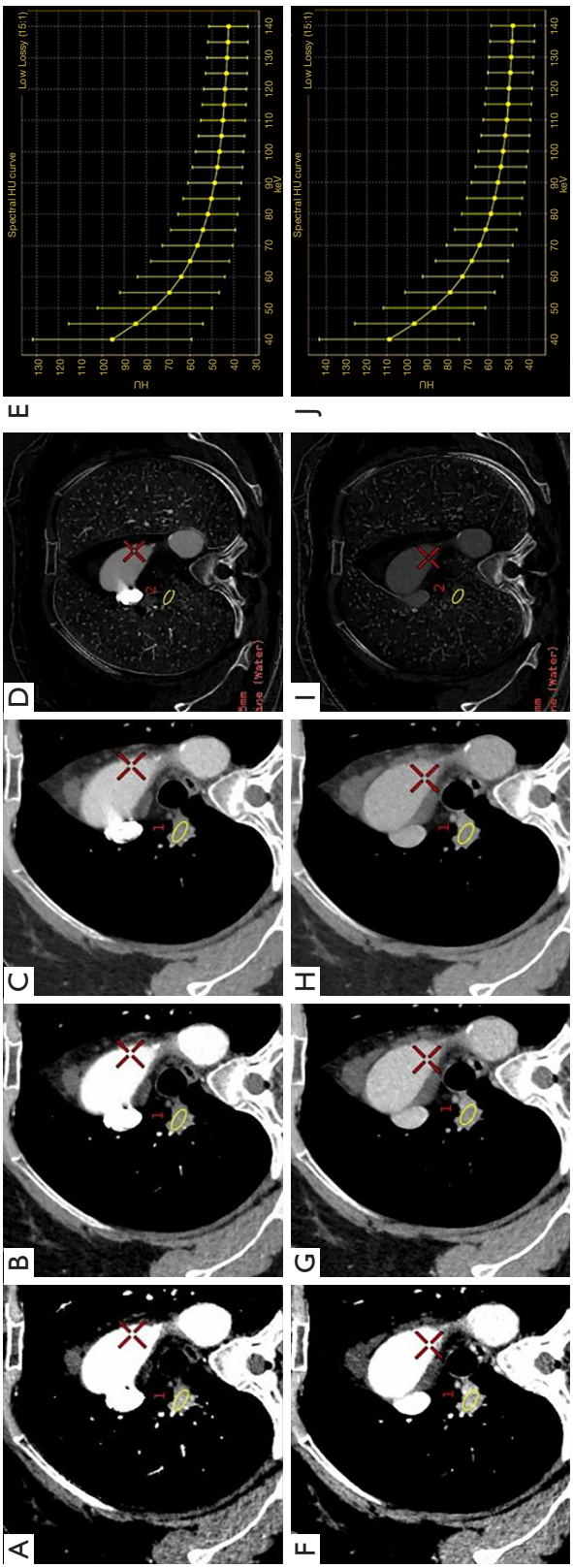

Figure 4 Spectral CT quantitative parameters in a 66-year-old female with LUAD with STAS. (A-E) Arterial phase; (F-J) venous phase. (A,F) CT40keV value is 95.48 and 108.84 HU, respectively; (B,G) CT70keV value is 56.63 and 64.30 HU, respectively; (C,H) CT100keVa value is 46.57 and 52.71 HU, respectively; (D,I) the IC of the lesion is 6.69×100 and 7.84×100 μg/cm^3, respectively; (E,J) spectral curve (λHU is 0.82 and 0.94, respectively). Yellow circles represent the regions of interest. HU, Hounsfield unit; CT, computed tomography; LUAD, lung adenocarcinoma; STAS, spread through air spaces; IC, iodine concentration; λHU, slope of the spectral curve.

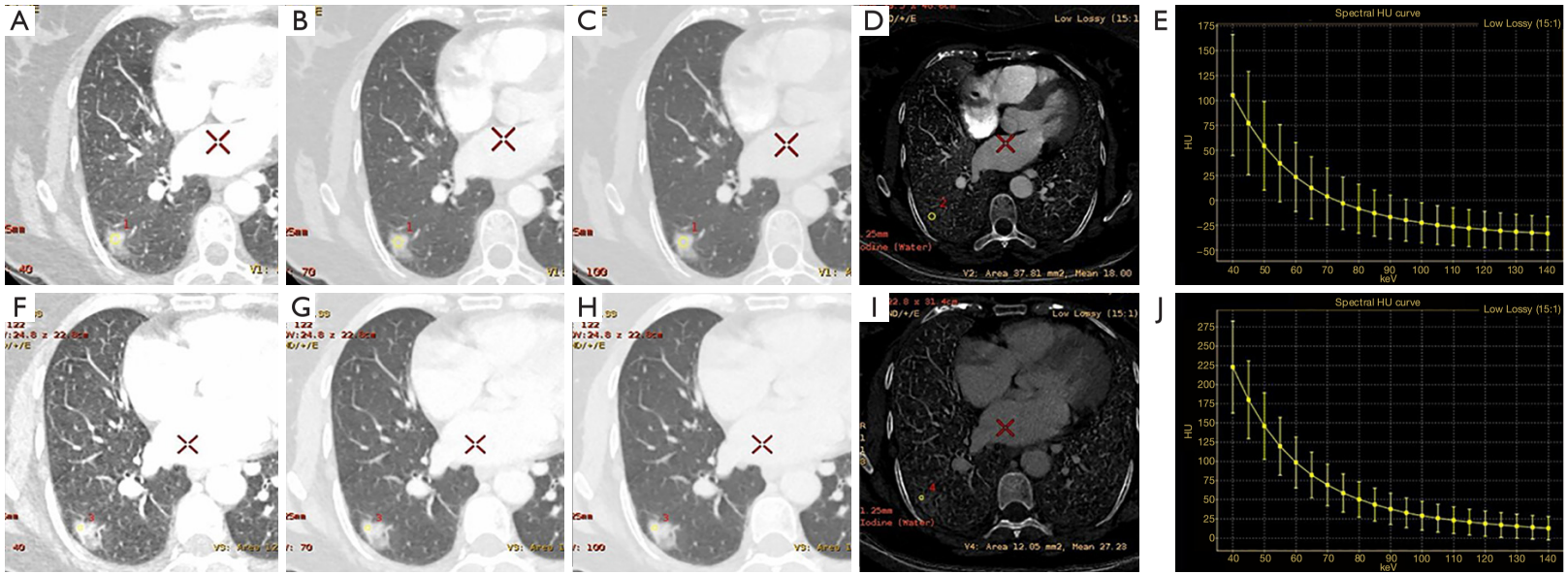

Figure 5 Spectral CT quantitative parameters in a 64-year-old female with lung adenocarcinoma without STAS. (A-E) Arterial phase; (F-J) venous phase. (A,F) CT40keV value is 105.42 and 222.91 HU, respectively; (B,G) CT70keV value is 3.84 and 69.23 HU, respectively; (C,H) CT100keVa value is –22.57 and 29.23 HU, respectively; (D,I) the IC of the lesion is 18.00×100 and 27.23×100 μg/cm^3, respectively; (E,J) spectral curve (λHU is 2.13 and 3.23, respectively). Yellow circles represent the regions of interest. HU, Hounsfield unit; CT, computed tomography; STAS, spread through air spaces; IC, iodine concentration; λHU, slope of the spectral curve.

supply to proliferate. The degree of tumor enhancement, as reflected by the CT value, can be used to measure the degree of tumor vascularization, thereby reflecting the blood supply of the tumor. Therefore, the findings of this study indirectly reflected the blood supply requirement of tumors exhibiting STAS.

Regarding the conventional CT signs, our study reveals that STAS-positive tumors were more likely to exhibit spiculation and a greater number of solid components, which is consistent with earlier studies (12,13). In contrast to the previous studies, our study did not observe a significant correlation between STAS and lobulation or pleural indentation. This deviation from the prior research results may be related to the sample size. Nevertheless, our results still indicated that STAS-positive tumors exhibited a higher incidence of lobulation and pleural indentation.

In order to quantitatively evaluate the lesions, many studies have adopted radiomics and achieved good results (22-24). Radiomics can extract a large number of quantitative features from images, which can reflect information that cannot be observed by the naked eye. However, our study provides a novel approach for clinical application aimed at establishing a new relationship between spectral CT quantitative parameters and STAS. Compared with conventional CT, spectral CT can quantitatively evaluate tumors using multiple parameters. Our research findings indicate that CT100keVa and CT100keVv can independently identify STAS status. This, to the best of our knowledge, is the first novel discovery that suggests the potential value of spectral CT quantitative parameters in identifying STAS in LUAD. Previous studies (13,25) have built models utilizing CT features to evaluate STAS in LUAD and achieved moderate predictive efficiency. In this study, the model based on the combination of conventional CT features and spectral CT quantitative parameters showed better discriminative ability, with an AUC of 0.952, sensitivity of 90.6%, and specificity of 86.7%, and outperformed their models. Combining qualitative and quantitative analysis represents a fantastic opportunity for clinicians to distinguish STAS-positive from -negative cases of LUAD.

Although the current study presented critical findings, it has some limitations. First, the sample size of this study was small, and more cases are necessary to validate our findings. Second, we did not examine the association between spectral CT parameters and STAS in various histologic subtypes of LUAD. Third, our study was restricted to a limited number of tumor layers and did not consider the overall characteristics of the lesion. Fourth, our study used a single CT scanner, and the findings need to be validated on different types of scanners.

Conclusions

Our study demonstrates a correlation between spectral CT quantitative parameters and STAS status in LUAD, with CT100keVa and CT100keVv exhibiting the potential for identifying STAS.

Acknowledgments

Funding: None.

Footnote

Reporting Checklist: The authors have completed the STARD reporting checklist. Available at https://qims.amegroups.com/article/view/10.21037/qims-23-984/rc

Conflicts of Interest: All authors have completed the ICMJE uniform disclosure form (available at https://qims.amegroups.com/article/view/10.21037/qims-23-984/coif). The authors have no conflicts of interest to declare.

Ethical Statement: The authors are accountable for all aspects of the work in ensuring that questions related to the accuracy or integrity of any part of the work are appropriately investigated and resolved. This study was conducted in accordance with the Declaration of Helsinki (as revised in 2013). The Institutional Ethics Committee of the Affiliated Hospital of Qingdao University approved the study (No. QYFY WZLL 28103), and the requirement for individual consent for this retrospective analysis was waived.

References

1. Sung H, Ferlay J, Siegel RL, Laversanne M,

Soerjomataram I, Jemal A, Bray F. Global Cancer Statistics 2020: GLOBOCAN Estimates of Incidence and Mortality Worldwide for 36 Cancers in 185 Countries. CA Cancer J Clin 2021;71:209-49.
2. Meza R, Meernik C, Jeon J, Cote ML. Lung cancer incidence trends by gender, race and histology in the United States, 1973-2010. PLoS One 2015;10:e0121323.
3. Travis WD, Brambilla E, Nicholson AG, Yatabe Y, Austin JHM, Beasley MB, Chirieac LR, Dacic S, Duhig E, Flieder DB, Geisinger K, Hirsch FR, Ishikawa Y, Kerr KM, Noguchi M, Pelosi G, Powell CA, Tsao MS, Wistuba I; . The 2015 World Health Organization Classification of Lung Tumors: Impact of Genetic, Clinical and Radiologic Advances Since the 2004 Classification. J Thorac Oncol 2015;10:1243-60.
4. Nicholson AG, Tsao MS, Beasley MB, Borczuk AC, Brambilla E, Cooper WA, Dacic S, Jain D, Kerr KM, Lantuejoul S, Noguchi M, Papotti M, Rekhtman N, Scagliotti G, van Schil P, Sholl L, Yatabe Y, Yoshida A, Travis WD. The 2021 WHO Classification of Lung Tumors: Impact of Advances Since 2015. J Thorac Oncol 2022;17:362-87.
5. Warth A, Muley T, Kossakowski CA, Goeppert B, Schirmacher P, Dienemann H, Weichert W. Prognostic Impact of Intra-alveolar Tumor Spread in Pulmonary Adenocarcinoma. Am J Surg Pathol 2015;39:793-801.
6. Dai C, Xie H, Su H, She Y, Zhu E, Fan Z, Zhou F, Ren Y, Xie D, Zheng H, Kadeer X, Chen D, Zhang L, Jiang G, Wu C, Chen C. Tumor Spread through Air Spaces Affects the Recurrence and Overall Survival in Patients with Lung Adenocarcinoma >2 to 3 cm. J Thorac Oncol 2017;12:1052-60.
7. Cao C, Chandrakumar D, Gupta S, Yan TD, Tian DH. Could less be more?-A systematic review and meta-analysis of sublobar resections versus lobectomy for non-small cell lung cancer according to patient selection. Lung Cancer 2015;89:121-32.
8. Okada M, Koike T, Higashiyama M, Yamato Y, Kodama K, Tsubota N. Radical sublobar resection for small-sized non-small cell lung cancer: a multicenter study. J Thorac Cardiovasc Surg 2006;132:769-75.
9. Ren Y, Xie H, Dai C, She Y, Su H, Xie D, Zheng H, Zhang L, Jiang G, Wu C, Chen C. Prognostic Impact of Tumor Spread Through Air Spaces in Sublobar Resection for 1A Lung Adenocarcinoma Patients. Ann Surg Oncol 2019;26:1901-8.
10. Kadota K, Nitadori JI, Sima CS, Ujiie H, Rizk NP, Jones DR, Adusumilli PS, Travis WD. Tumor Spread through Air Spaces is an Important Pattern of Invasion and Impacts the Frequency and Location of Recurrences after Limited Resection for Small Stage I Lung Adenocarcinomas. J Thorac Oncol 2015;10:806-14.
11. Li C, Jiang C, Gong J, Wu X, Luo Y, Sun G. A CT-based logistic regression model to predict spread through air space in lung adenocarcinoma. Quant Imaging Med Surg 2020;10:1984-93.
12. Toyokawa G, Yamada Y, Tagawa T, Kamitani T, Yamasaki Y, Shimokawa M, Oda Y, Maehara Y. Computed tomography features of resected lung adenocarcinomas with spread through air spaces. J Thorac Cardiovasc Surg 2018;156:1670-1676.e4.
13. Qin L, Sun Y, Zhu R, Hu B, Wu J. Clinicopathological and CT features of tumor spread through air space in invasive lung adenocarcinoma. Front Oncol 2022;12:959113.
14. Gu Y, Zheng B, Zhao T, Fan Y. Computed Tomography Features and Tumor Spread Through Air Spaces in Lung Adenocarcinoma: A Meta-analysis. J Thorac Imaging 2023;38:W19-29.
15. Wu F, Zhou H, Li F, Wang JT, Ai T. Spectral CT Imaging of Lung Cancer: Quantitative Analysis of Spectral Parameters and Their Correlation with Tumor Characteristics. Acad Radiol 2018;25:1398-404.
16. González-Pérez V, Arana E, Barrios M, Bartrés A, Cruz J, Montero R, González M, Deltoro C, Martínez-Pérez E, De Aguiar-Quevedo K, Arrarás M. Differentiation of benign and malignant lung lesions: Dual-Energy Computed Tomography findings. Eur J Radiol 2016;85:1765-72.
17. Lin LY, Zhang Y, Suo ST, Zhang F, Cheng JJ, Wu HW. Correlation between dual-energy spectral CT imaging parameters and pathological grades of non-small cell lung cancer. Clin Radiol 2018;73:412.e1-7.
18. Yang F, Dong J, Wang X, Fu X, Zhang T. Non-small cell lung cancer: Spectral computed tomography quantitative parameters for preoperative diagnosis of metastatic lymph nodes. Eur J Radiol 2017;89:129-35.
19. Masai K, Sakurai H, Sukeda A, Suzuki S, Asakura K, Nakagawa K, Asamura H, Watanabe SI, Motoi N, Hiraoka N. Prognostic Impact of Margin Distance and Tumor Spread Through Air Spaces in Limited Resection for Primary Lung Cancer. J Thorac Oncol 2017;12:1788-97.
20. Toyokawa G, Yamada Y, Tagawa T, Kozuma Y, Matsubara T, Haratake N, Takamori S, Akamine T, Oda Y, Maehara Y. Significance of Spread Through Air Spaces in Resected Pathological Stage I Lung Adenocarcinoma. Ann Thorac Surg 2018;105:1655-63.

21. Vaghjiani RG, Takahashi Y, Eguchi T, Lu S, Kameda K, Tano Z, Dozier J, Tan KS, Jones DR, Travis WD, Adusumilli PS. Tumor Spread Through Air Spaces Is a Predictor of Occult Lymph Node Metastasis in Clinical Stage IA Lung Adenocarcinoma. J Thorac Oncol 2020;15:792-802.
22. Bassi M, Russomando A, Vannucci J, Ciardiello A, Dolciami M, Ricci P, Pernazza A, D'Amati G, Mancini Terracciano C, Faccini R, Mantovani S, Venuta F, Voena C, Anile M. Role of radiomics in predicting lung cancer spread through air spaces in a heterogeneous dataset. Transl Lung Cancer Res 2022;11:560-71.
23. Liao G, Huang L, Wu S, Zhang P, Xie D, Yao L, Zhang Z, Yao S, Shanshan L, Wang S, Wang G, Wing-Chi Chan L, Zhou H. Preoperative CT-based peritumoral and tumoral radiomic features prediction for tumor spread through air spaces in clinical stage I lung adenocarcinoma. Lung Cancer 2022;163:87-95.
24. Han X, Fan J, Zheng Y, Ding C, Zhang X, Zhang K, Wang N, Jia X, Li Y, Liu J, Zheng J, Shi H. The Value of CT-Based Radiomics for Predicting Spread Through Air Spaces in Stage IA Lung Adenocarcinoma. Front Oncol 2022;12:757389.
25. Qi L, Xue K, Cai Y, Lu J, Li X, Li M. Predictors of CT Morphologic Features to Identify Spread Through Air Spaces Preoperatively in Small-Sized Lung Adenocarcinoma. Front Oncol 2020;10:548430.

Cite this article as: Song H, Cui S, Zhang L, Lou H, Yang K, Yu H, Lin J. Preliminary exploration of the correlation between spectral computed tomography quantitative parameters and spread through air spaces in lung adenocarcinoma. Quant Imaging Med Surg 2024;14(1):386-396. doi: 10.21037/qims-23-984

